Pt-induced nanowires on Ge(001): *Ab initio* study

A. A. Stekolnikov,* J. Furthmüller, and F. Bechstedt
Institut für Festkörpertheorie und -optik, Friedrich-Schiller-Universität and European Theoretical Spectroscopy Facility (ETSF), Max-Wien-Platz 1, 07743 Jena, Germany
(Received 24 June 2008; published 28 October 2008)

Using *ab initio* density-functional theory together with a semilocal approximation for exchange and correlation we study structural, energetical, and electronic properties for a variety of reconstruction models of the Ge(001)4×2 surface with a Pt coverage of 0.25 monolayer. The band-structure calculations are partially performed including spin-orbit interaction. Starting from the idea that the self-organization of the nanowire arrays is driven by the minimization of the total energy of the system, we investigate more than 20 possible overlayer structures, among them dimerized top Pt chains. The comparison of the surface energies, however, shows a clear preference of the formation of Pt-Ge bonds over Pt-Pt bonds. The most favorable surface structure contains fourfold-coordinated Pt atoms embedded in Ge atoms. The seemingly dimerized top chains are formed by edges of Ge tetramers parallel to Ge dimers in trenches two atomic layers below. Incorporation of Pt atoms in the surface Ge layer within the tetramer-dimer-chain model gives rise to the biggest energy gain. Its band structure describes an indirect semiconductor with almost vanishing gap. The role of the Pt 5*d* states and top-ridge Ge orbitals as well as of spin-orbit interaction is emphasized for the wire conductivity. The results are discussed in light of recent experimental scanning-tunneling microscopy studies.

DOI: 10.1103/PhysRevB.78.155434 PACS number(s): 68.35.−p, 68.37.Ef, 68.43.Bc, 73.20.At

I. INTRODUCTION

True one-dimensional (1D) electronic systems have attracted great interest because of their expected exotic electronic properties, which include charge-density wave (CDW), spin-density wave (SDW), triplet superconductivity, and Luttinger-liquid (LL) behavior.[1,2] Properties of electrons related to charge and spin may be separated in a quasiparticle picture.[2,3] In a LL the electron loses its identity and separates into two quasiparticles. In a photoemission experiment the excitation should decay into a spinon that carries spin without charge and a holon that carries the positive charge of a hole without its spin.[3] Metal chains of clear 1D character should exhibit a Peierls instability[4] which results in a phase transition accompanied by a change in the translational symmetry and a gap opening.[5] In metallic chains, electrons and holes near the Fermi energy often couple strongly with lattice vibrations, thereby generating a periodic spatial modulation of charge, i.e., a CDW which may also open a band gap, a CDW gap.[1,6] In this respect self-organized quasi-1D surface structures induced by metal adsorption on semiconductor surfaces[7–9] have attracted enormous attention during the last decade. Besides possible future applications the interest is driven by the wealth of novel exotic physical phenomena which are possibly observable also in quasi-1D systems.

Prototypical examples for metal-induced chain structures on semiconductor substrates are In/Si(111), Au/Si(111), Pt/Ge(001), and Au/Ge(001) systems.[7–10] Sometimes one can tailor the electronic states[11] or conductivity within temperature-induced phase transitions.[12] Metal nanowires also have attracted special interest because of their electric transport properties. The 5*d* noble metals Ir, Pt, and Au tend to form surface reconstructions containing chains on their low-index surfaces[13] in contrast to 4*d* metals such as Pd which do not give rise to ordered chains.[14] The central problem of the understanding of electronic and transport properties is the knowledge of the underlying atomic geometries and their possible modification due to external conditions, e.g., temperature.[15,16] Recent experiments reported the observation of metallic chains on Ge(001) and Si(001) substrates after Pt or Au deposition.[9,10,14–18] However, the chain formation and the bonding mechanism are still under debate. In particular, the role of the metal 5*d* states is controversially discussed for the incorporation and subsequent coordination of the noble metal atoms. The common picture is that the strong relativistic character of the 5*d* states leads to a preference for the low coordination of Au, Pt, and Ir atoms and, hence, the formation of dimerized chains instead of cluster formation.[10,13,14,16]

Most interesting is the behavior of a quarter of a monolayer of Pt atoms on a Ge(001) surface. However, the adsorption mechanism—the incorporation of the Pt atoms into the Ge substrate or the on-top deposition of the metal atoms—is under discussion.[17] The conventional picture of quasi-1D arrays contains linear chains of dimerized Pt atoms.[9] Even the controlled local demolition and repair of such wires is explained in terms of on-top Pt dimers.[19] In addition, the role of the Pt atoms for the formation of electronic states near the Fermi level as well as the role of quantum-mechanical confinement effects are not clarified.[18,20] The same holds for the asymmetry of the chain structure and the disappearance of the dimerization for low bias voltages.[16,18] There are also differences in the measured electronic structures. This holds for the substantial redistribution of the differential conductivity (dI/dV) versus voltage of Pt-induced nanowires after cooling down to liquid-nitrogen temperature[16] but also for remarkable discrepancies of the room-temperature results of two different experimental groups.[16,18] Another open question is the nature of the peak in the differential conductivity just above the Fermi level. Recently, it has been interpreted as the consequence of quantum confinement of empty electronic states between two nanowires.[16,20] However, also another interpretation toward unfilled antibonding Pt-Ge states

is possible. Recently, in a joint letter of theoretical and experimental colleagues[21] with two authors (Stekolnikov and Bechstedt) of the present paper it has been suggested a completely new structure with buried Pt-Ge chains which may explain the scanning-tunneling microscopy (STM) images in a wide bias range, including energies around the Fermi level.

In this paper we study the formation of quasi-1D chains on the Pt/Ge(001) surface by means of total-energy and electronic-structure calculations in detail. The computational methods are described in Sec. II. The different model structures and the accompanying band structures are presented and discussed in Secs. III–V. Finally, in Sec. VI a summary and conclusions are given.

II. CALCULATIONAL METHODS

The total energies, the optimized atomic geometries, and a first approach to the electronic structures are calculated within the density-functional theory (DFT) (Ref. 22) in a semilocal approximation for the exchange-correlation (XC) functional.[23] The generalized gradient approximation (GGA) (Refs. 24 and 25) allows for a better description of more long-range interactions. At this stage of computations no spin polarization is taken into account. Explicitly, we use the Vienna *ab initio* simulation package (VASP) code.[26] The pseudopotentials are generated within the projector augmented wave (PAW) method[27] which allows for a substantial reduction of the plane-wave cutoff to 18.4 Ry. According to the test calculations, the cutoff is chosen somewhat larger than in the case of clean Ge surfaces.[28] It is also sufficient for the treatment of the Pt metal. The ground-state configurations of the outermost electrons in the free atoms are $4s^2 4p^2$ (Ge) and $5d^{10} 6s^0$ (Pt).

The **k**-space integrations for total energies and electron densities are replaced by summations over Monkhorst-Pack (MP) meshes.[29] The total energies depend on the coordinates of the Ge and Pt cores. For a given starting arrangement of the cores the equilibrium atomic geometry is obtained by relaxing the coordinates until the Hellmann-Feynman forces are less than 10 meV/Å. For bulk Ge, this procedure yields to a lattice constant of $a_0=5.760$ Å. The resulting bond length $d=2.49$ Å is about 1.7% larger than the experimental one due to the underbinding within the DFT-GGA treatment. The corresponding indirect fundamental gap E_g amounts to $E_g=0.00$ eV if taken from the Kohn-Sham (KS) eigenvalues of the DFT.[23] This value is opened in the slab approximation to 0.16 eV due to quantum confinement effects. This results in a chemical potential (negative cohesive energy per atom) of $\mu_{\mathrm{Ge}}=-4.53$ eV. The corresponding values for a fcc Pt metal are $a_0=3.99$ Å and $\mu_{\mathrm{Pt}}=-6.02$ eV.

The Ge(001) surface is simulated by repeated asymmetric slabs with eight Ge bilayers and a vacuum region of the same extent.[28] Five of the eight atomic layers are allowed to relax. The bottom side of each slab with fixed atomic positions is saturated by hydrogen (H) atoms to simulate the continuation into the Ge bulk. The surface translational symmetry is determined by the Pt coverage. Experimental studies[16,18,20] typically indicate a 0.25-monolayer Pt coverage. This suggests studying 4×2 surface unit cells with two Pt atoms. The resulting translational symmetry corresponds nominally to eight Ge atoms in one bulklike (001) atomic layer of the substrate. In the case of the clean Ge(001) surface one cell would contain two rows of Ge dimers in $[1\bar{1}0]$ direction with a total of four dimers in the unit cell. The **k**-space integrations for total energies and densities are performed with a 4×8 MP mesh, i.e., 32 **k** points in the surface Brillouin zone (BZ). Using a variety of starting atomic geometries representing a certain adsorbate model several model structures have been tested and compared with respect to their total energy. More precisely, we compare surface formation energies of the form (per surface unit cell)

$$\Omega_f = E_{\mathrm{slab}}(N_{\mathrm{Ge}},N_{\mathrm{Pt}},N_{\mathrm{H}}) - \mu_{\mathrm{Ge}}N_{\mathrm{Ge}} - \mu_{\mathrm{Pt}}N_{\mathrm{Pt}} - \mu_{\mathrm{H}}N_{\mathrm{H}}, \quad (1)$$

with E_{slab} as the total energy of the slab containing $N_{\mathrm{Ge}}(N_{\mathrm{Pt}},N_{\mathrm{H}})$ Ge(Pt, H) atoms. There may be a particle exchange with reservoirs described by the corresponding chemical potentials $\mu_{\mathrm{Ge}}(\mu_{\mathrm{Pt}},\mu_{\mathrm{H}})$. Since definition (1) gives the formation energy of both surfaces of the slabs (including the hydrogen-passivated one, in which we are not interested), we only study a relative formation energy of the Pt-covered systems

$$\Delta\Omega_f = E_{\mathrm{slab}}(N_{\mathrm{Ge}},N^0_{\mathrm{Pt}},N^0_{\mathrm{H}}) - E_{\mathrm{slab}}(N^0_{\mathrm{Ge}},N^0_{\mathrm{Pt}},N^0_{\mathrm{H}}) - \mu_{\mathrm{Ge}}(N_{\mathrm{Ge}}-N^0_{\mathrm{Ge}}), \quad (2)$$

with respect to a certain adsorbate with the atomic numbers N^0_{Ge}, N^0_{Pt}, and N^0_{H}. Since the number of Pt atoms, $N^0_{\mathrm{Pt}}=2$, and the number of H atoms, $N^0_{\mathrm{H}}=16$, do not vary, the relative formation energy (2) only depends on the chemical potential of the N_{Ge} Ge atoms.

The eigenvalues and eigenfunctions of the Kohn-Sham equation[23] are used to calculate electronic properties such as electron densities, total electronic densities of states, energy-resolved local electronic densities of states (more precisely, STM images within the Tersoff-Hamann approach[30]), and even band structures. However, these quantities do not account for the excitation aspect.[31–33] Interband excitation energies and gaps in the band structure are considerably underestimated. For instance, the DFT-GGA gap has to be corrected by quasiparticle corrections. Within a perturbation-theory approach they open the fundamental gap of Ge bulk by about 0.6–0.7 eV (Refs. 31–33) in agreement with the measured value. On the other hand, the quasiparticle corrections should vanish at the Fermi energy.[33] Since we focus our studies to single-particle energies not too far from the Fermi energy, we neglect the quasiparticle corrections in the computations of band structures and STM images. However, because of the high atomic number $Z=78$ of Pt the spin-orbit (SO) interaction may influence the band structure and density of states (DOS). Therefore, we take into account the spin-orbit coupling in the band-structure calculation for the most interesting and energetically favorable adsorbate-structure model. The studies with SO interaction are based on the von Barth and Hedin's local spin-density theory for exchange and correlation[34] which are generalized to the treatment of noncollinear arrangements. The basic idea is to investigate locally a system with defined spin density. The noncollinearity is treated by transformation of the local co-

TABLE I. Relative surface formation energy [Eq. (2)] in meV/1×1 unit cell for the Pt/Ge(001) adsorbate systems with fixed Pt number $N_{Pt}=2$ per 4×2 unit cell and fixed H number $N_H=16$ per asymmetric slab. The number of Ge atoms N_{Ge} varies.

Model	Number N_{Ge}	Relative formation energy $\Delta\Omega_f$
HD2 [Fig. 1(a)]	64	0
HD4 [Fig. 1(b)]	64	81
HDR [Fig. 5(a)]	64	383
HRT [Fig. 5(b)]	58	178
MDN [Fig. 6(a)]	64	−20
MDS [Fig. 6(b)]	64	−104
HDT [Fig. 6(c)]	64	−48
SHD (Not shown)	62	−103
SMD [Fig. 7(a)]	62	−205
SMA [Fig. 7(b)]	62	−200
SMR [Fig. 7(c)]	58	−211
BDN [Fig. 8(a)]	64	−70
BDS [Fig. 8(b)]	64	−132
BDA [Fig. 8(c)]	64	−151
BDC [Fig. 8(d)]	64	−181
BDP [Fig. 8(e)]	64	−178
TDC (Fig. 9)	62	−250

ordinate system. Such a generalization for noncollinear spin systems has been recently implemented within the PAW method in the VASP code.[35] It also allows the calculation of electronic structures with spin-orbit interaction. The valence-band maximum of the diamond-structure Ge crystal is given by sixfold-degenerate (including spin) $\Gamma_{25'}$ (mainly $4p$-derived) states which split into fourfold-degenerate Γ_8 and twofold Γ_7 levels due to spin-orbit interaction.[36] We calculate a bulk level separation $\Delta_{SO}=0.29$ eV for Ge in excellent agreement with the experimental value.[37]

Keeping the idea of a 0.25-monolayer Pt coverage we have studied more than 20 different reconstruction models by means of total-energy calculations. Most of them are directly compared in Table I with respect to their relative surface formation energy [Eq. (2)]. For many of these reconstructions we present figures of their stick-and-ball models of the atomic geometries. For a few, the energetically most favorable models, important bond lengths are shown. For the majority of these also the electronic structure is discussed. The electronic structure is characterized by elements such as the band structure (without and with spin-orbit interaction) versus high-symmetry lines in the surface BZ, wave-function squares, the DOS, and STM images. The results are discussed in light of the available experimental data. The presentation is divided in groups of adsorbate models in accordance to the type of occurring bonds, Pt-Pt and Pt-Ge ones, and the position of the Pt atoms.

III. PT HOMODIMER CHAINS ON TOP OF Ge(001) SURFACE

A. Geometry and bonding

First, we follow the idea of formation of Pt-Pt homodimers on top of a dimerized Ge(001) surface with Ge dimer rows parallel to the $[1\bar{1}0]$ direction. Such models are suggested by the observed STM images representing parallel chains in a distance of 16 Å and chain links with an extent of 8 Å.[16–18,20] In Fig. 1 the homodimer-2 (HD2) model (a) contains Pt pairs which bridge two Ge dimers in the same dimer row. In the case of the homodimer-4 (HD4) model (b) a pair of Pt atoms bridges pairs of two dimers belonging to two adjacent rows of Ge dimers in [110] direction. The formation of Pt-Ge bonds between first and second atomic layers requires the break of the π bonds of the substrate dimers involved in the bridging process. The resulting characteristic bond lengths are also presented in Fig. 1. They are with 2.31–2.39 Å much shorter than bulk Ge-Ge bonds. The lengths 2.72–2.73 Å of the Pt-Pt bonds approach twice of the radius 1.39 Å of a Pt ion.[38] The lengths of the Ge-Ge bonds of the former dimers in Fig. 1(b) are difficult to determine because of the corresponding flat minimum on the total energy surface.

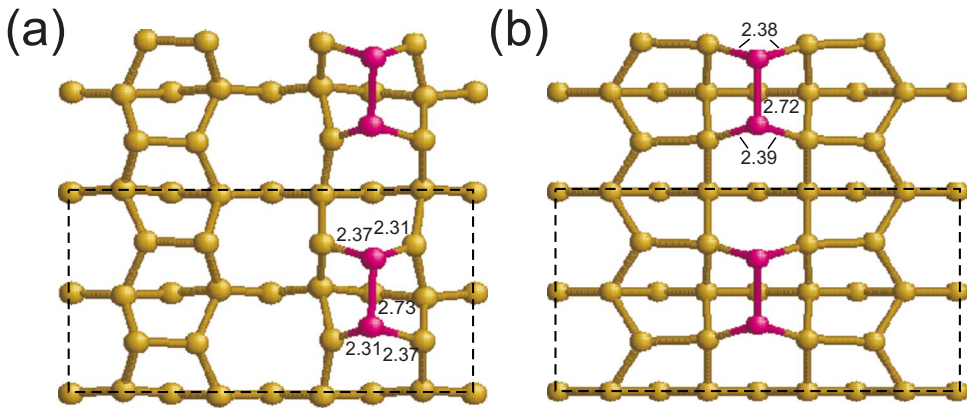

FIG. 1. (Color online) Dimerized Ge(001) surface (top view) with top Pt-Pt homodimers on top parallel to $[1\bar{1}0]$: bridging two Ge dimers in one and the same row (HD2 structure) (a) or pairs of two dimers belonging to neighboring rows (HD4 structure) (b). Both adsorbates give rise to a 4×2 reconstruction as indicated by the unit cell (dashed lines). In the stick-and-ball model the bright (yellow) spheres indicate Ge atoms while the dark (red) spheres describe Pt atoms. Characteristic bond lengths (in Å) are indicated by numbers.

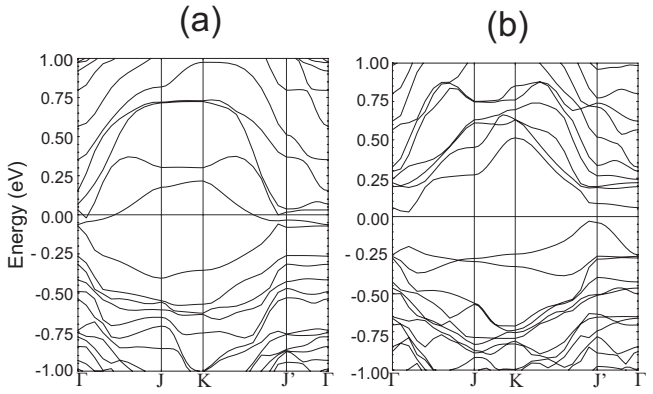

FIG. 2. Band structures of the Pt homodimer models shown in Fig. 1. The Fermi level is used as energy zero. The BZ is explained in Ref. 39.

The Pt-Pt but especially the Pt-Ge bonds stabilize the adsorbate structures. The formation energies of the two Pt homodimer models in Table I are rather similar. The bridging of two Ge dimers in one row is slightly energetically favored by 81 meV/1×1 unit cell. This fact is not surprising since the HD2 model does not possess Ge dangling bonds contrary to the HD4 model. Both models can explain the dimerized chains observed in STM images,[16–18,20] but not the asymmetry of these images perpendicular to the chain direction.

B. Metallic or insulating character

Despite the similarities of the top Pt homodimers in Fig. 1, the resulting band structures in Fig. 2 exhibit drastic differences. The HD2 structure clearly gives rise to a metallic overlayer due to Pt states at the Fermi level [Fig. 2(a)]. The dimerization of the linear Pt chains parallel to $[1\bar{1}0]$ is not strong enough. Because of the interaction with the substrate atoms the Peierls effect[4] is weakened. The situation is different for the Pt homodimers bridging two different Ge dimer rows. The Peierls distortion of the linear Pt chains related to the dimerization leads to a metal-insulator transition. In Fig. 2(b) an indirect gap appears with the conduction-band minimum (CBM) near the Γ point while the valence-band maximum (VBM) occurs near J'. Surprisingly the semiconducting HD4 geometry is somewhat higher in total energy (cf. Table I) than the metallic HD2 structure. The reason is the fact that the Ge atoms of the former dimers farthest away from the Pt chains form too long bonds with the Ge atoms of the second layer. This gives rise to a surface stress which is larger than that in the clean Ge(001) surface.

The indirectness of the band structure is a consequence of the strong dispersion of the Pt-derived bands along the chain direction $[1\bar{1}0]$, i.e., ΓJ and KJ'. For the illustration of the origin we have shown the variation in the orbital character of the lowest conduction band in Fig. 3. Along ΓJ it contains strong contributions from the antibonding Ge σ dimer states but also significant Pt d and s contributions belonging to the Pt-Ge bonds are visible in Figs. 3(a) and 3(b). Changing to the BZ boundary near J' the contributions from the Ge dimers states disappear. Empty Pt $5d$ (e_g) states dominate the CBM [see Fig. 3(c)]. We note that even a different orbital character of the Pt d states is visible with, e.g., $3z^2-r^2$ (z parallel to $[1\bar{1}0]$) in Fig. 3(c). States of Pt d origin also substantially contribute to the VBM in Fig. 2(b). However, Fig. 3(d) also shows strong contributions from filled Ge bonding states located between Ge atoms of the former dimer rows opposite to the Pt dimers.

Nevertheless, surprisingly the Pt states give the main contributions to the STM images for occupied states until 1 eV below the Fermi level in Fig. 4. The reason is not only that the two uppermost valence bands at about −0.25 eV in Fig. 2(b) have a strong Pt d character. Electrons are transferred from the Ge dangling bonds and populate Pt states at the threefold-coordinated Pt atoms. The lower-lying Ge-derived states belonging to the bands in the range −1.00… −0.25 eV are not visible in Fig. 4 because a plane above the top Pt atoms is chosen to plot the STM image. Taking the same distances to the Pt atoms the other Pt-Pt homodimer structure shown in Fig. 1(a) gives rise to similar STM images (not shown) which may be interpreted as dimerized Pt chains in the top atomic layer.

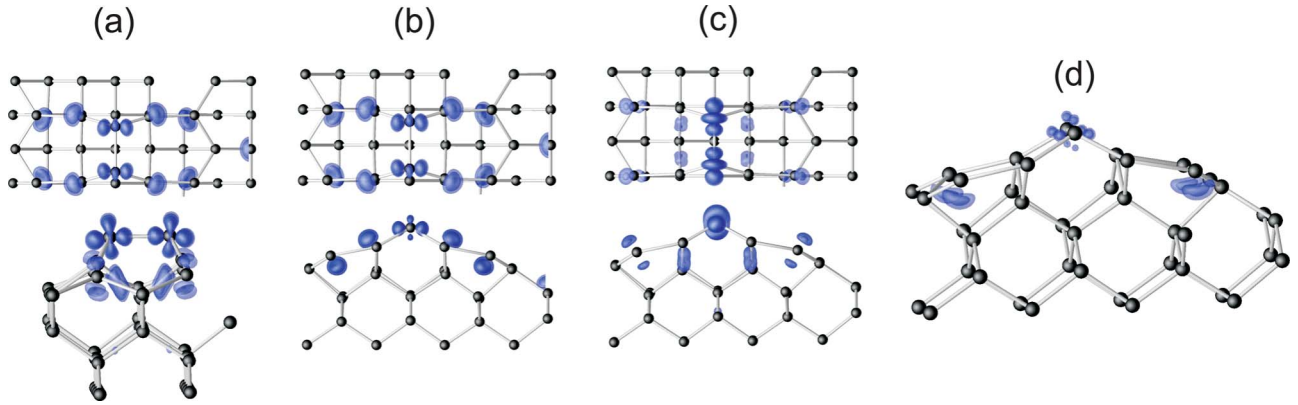

FIG. 3. (Color online) Wave-function squares (top and side views) of the lowest conduction-band states at Γ (a), J (b), and close to J' (c) in the band structure of Fig. 2(b) for the homodimer model in Fig. 1(b). In addition, the wave-function square of the state at the VBM near J' (d) is also plotted. In the lower panel of (a) and in (d) perspective views are shown. The probabilities are indicated by blue clouds while dots represent atomic cores.

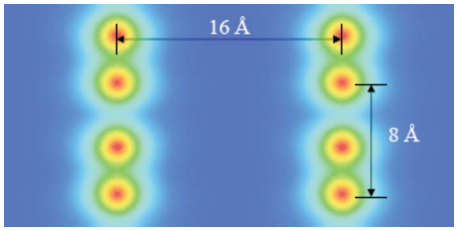

FIG. 4. (Color online) STM images simulated for the Pt dimer models in Fig. 1(b) for a bias voltage of −1 V (occupied states) for four unit cells. The constant-height images are plotted in a plane 3 Å above the topmost Pt atoms. Characteristic distances between parallel Pt chains (16 Å) and between two dimers within one chain (8 Å) are also given.

IV. REFINEMENTS OF DIMER-CHAIN STRUCTURES

A. Refinements of homodimer models: Modification of underlying ring structure

Chain structures such as the quasi-1D overlayers on the In/Si(111)4×1 (Ref. 40) are accompanied by a modification of the sixfold ring structures known from bulk tetrahedrally coordinated crystals. The homodimer models (Fig. 1) can be also refined by the formation of five- and sevenfold rings (Fig. 5) instead of six-member bond rings similar to the chain structures suggested for the Bi/Si(001) adsorbates.[41,42] Linear chains of Pt atoms still stay on top in a distance of about 16 Å. However, according to our computations all the studied rebonded ring structures are energetically less favorable than the adsorbate geometries in Fig. 1 (see Table I). We conclude that a change in the ring structure does not tend to reduce the total energy contrary to the situation in the Bi/Si(001) system. The reason is that the difference of the covalent radii of Bi and Si is much larger than that for Pt and Ge.[43]

B. Threefold-coordinated Pt atoms: Pt-Ge heterodimers and Ge homodimers

In the following approach for the adsorbate we allow an exchange of Ge and Pt atoms in a geometry similar to that of a homodimer model as indicated in Fig. 6. Thereby we only study the HD2 structure [Fig. 1(a)] as a starting point since the HD4 one [Fig. 1(b)] is energetically less favorable. The exchange reaction leads to threefold-coordinated Pt atoms in the top atomic layer as well as in the layer below. In the two resulting heterodimer structures Pt-Pt bonds occur [Fig. 6(a)], or Pt-Ge bonds of threefold-coordinated Pt atoms surrounded by Ge atoms result [Fig. 6(b)]. We call the two models mixed dimer with neighboring Pt atoms (MDN) and mixed dimer with second-nearest-neighbor Pt atoms (MDS). A continuation of the Pt-Ge exchange may lead to Ge homodimers on top, e.g., with the two Pt atoms in a third-nearest-neighbor position [Fig. 6(c)]. We call this model homodimer with Pt atoms in third-nearest-neighbor position (HDT).

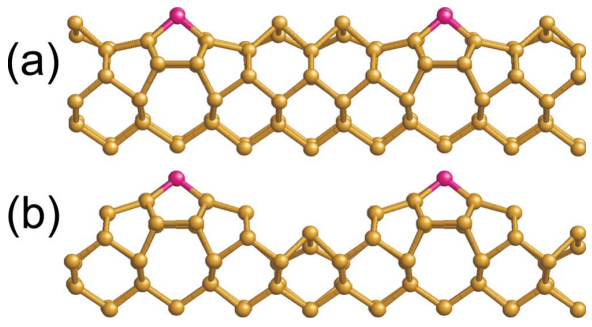

FIG. 5. (Color online) Stick-and-ball models of homodimer models with on-top Pt chains shown in Fig. 1 with modified Ge ring structures below (side view). The homodimer-modified ring (HDR) structure (a) is combined in (b) with the formation of a trench between the linear Pt chains due to desorption of Ge atoms. The structure (b) is therefore called homodimer-ring-trench (HRT) model. The bright (yellow) spheres describe Ge atoms while the dark (red) spheres stand for Pt atoms.

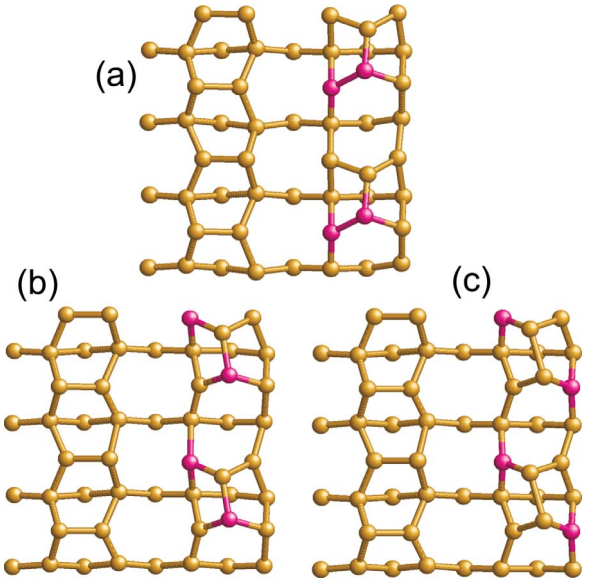

FIG. 6. (Color online) Dimerized Ge(001) surface with bridging dimers on top of one original dimer row. In contrast to the HD2 model in Fig. 1(a) Pt atoms in the top dimer and Ge neighbors from the layer below are exchanged. The (a) MDN, (b) MDS, and (c) HTD structures are shown. In the stick-and-ball model the bright (yellow) spheres describe Ge atoms while the dark (red) spheres stand for Pt atoms.

Interestingly the Pt-Ge heterodimer models MDN and MDS as well as the Ge homodimer HDT model gain energy in comparison to the Pt homodimers on top (see Table I). Thereby the energy lowering is larger if Pt-Pt bonds do not occur. This tendency is clearly visible by comparison of the two mixed-dimer structures in Figs. 6(a) and 6(b). The replacement of a pair of Pt-Pt and Ge-Ge bonds by two Pt-Ge bonds gains an energy of 84 meV (cf. Table I).

Despite the energetic favorization of the models in Fig. 6 compared to those in Fig. 1 intuitively constructed from the STM findings, the corresponding geometries shown in Fig. 6 can hardly explain the STM observations.[9,16,18] The three adsorbate geometries also describe parallel wires with a distance of about 16 Å and with a distance of the wire sections of 8 Å. The pairs of Pt and Ge or two Ge atoms on top may also represent the observed "dimerization." However, the top pair structures in Fig. 6 exhibit strong asymmetries, top

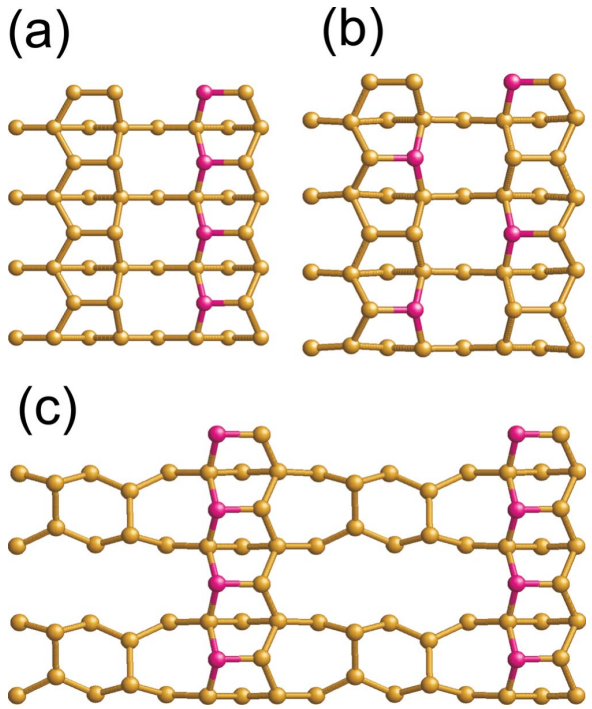

FIG. 7. (Color online) Dimerized Ge(001) surface with replacement of two Ge atoms (bright or yellow spheres) by Pt atoms (dark or red spheres). The stick-and-ball models correspond to the (a) SMD, (b) SMA, and (c) SMR structures.

dimer buckling or twisting, which have not been seen in measured STM images. The heterodimer in Fig. 6(a) is buckled whereas the top pair atoms are considerably displaced in the direction perpendicular to the chain direction [Figs. 6(b) and 6(c)]. The situation for a fourth thinkable model of the type presented in Fig. 6(c), Ge homodimers with the two Pt atoms in second-nearest-neighbor positions (not shown) would lead to similarly strong asymmetries. Only the asymmetry would be related to a strong dimer buckling instead of a lateral displacement of the dimer atoms. The energy gain is similar to that for the MDS model (see Table I).

C. Pt substitution into dimerized Ge(001) surface

In the next group of adsorbate structures we follow the idea of replacement of Ge atoms by Pt atoms and formation of threefold-coordinated Pt atoms surrounded only by Ge atoms as stabilizing elements for the Pt/Ge(001) adsorbate structure [see Fig. 6(b)]. These structural elements can easily be realized by substitution of Pt atoms in sites of the Ge dimers on top of a clean, dimerized Ge(001) surface. Three different possibilities for such a Pt substitution of two Ge dimer atoms in a 4×2 unit cell are shown in Figs. 7(a)–7(c). We call these models substitutional homodimer (SHD) [not shown; see clean Ge(001) surface], substitutional mixed dimer (SMD) [Fig. 7(a)], and substitutional mixed dimer in antiphase arrangement (SMA) [Fig. 7(b)]. In addition, in the SMD model we allow the removal (R) of the remaining top row of Ge dimers [Fig. 7(c)]. This model may be denoted by SMR.

Interestingly all substitutional dimer models give rise to an energy gain with respect to the top homodimer reconstructions in Fig. 1. We calculate larger energy gains than for the mixed-dimer models in Fig. 6 as obvious from Table I. This is especially valid if the Pt atoms occur in mixed dimers and hence form linear chains along the original dimer rows [Figs. 7(a) and 7(b)]. Surprisingly, the removal of each second dimer row of the clean Ge(001) surface and the formation of a trench between two mixed-dimer rows [Fig. 7(c)] seem to tend for a further lowering of the surface formation energy in Eq. (2).

The substitutional dimers in the SHD model (not shown) give rise to the smallest energy gain. Moreover, this model cannot explain the linear-chain character found experimentally.[9,16,18] The same holds for the SMA model [Fig. 7(b)]. The SMD model [Fig. 7(a)] is also in disagreement with STM observations because of still two parallel dimer rows in one unit cell. The characteristic distances 16 and 8 Å found in STM images appear only in the SMR model [Fig. 7(c)].

D. Bridging dimers and Pt-Ge exchange

In the models presented in Fig. 8 we have combined the idea of additional dimers on top of a dimerized surface, which bridge two pairs of dimers in parallel rows similar to the adsorbate system in Fig. 1(b), together with an exchange of Pt and Ge atoms. Resulting bridge dimer models with Pt atoms in nearest-neighbor (BDN model) or in second-nearest-neighbor (BDS model) positions are shown in Fig. 8(a) and Fig. 8(b), respectively. Further Pt-Ge exchange leads to pure bridging Ge-Ge dimers on top with an asymmetric arrangement [BDA model; see Fig. 8(c)], a chain arrangement [BDC model; see Fig. 8(d)], or a perpendicular arrangement [BDP model; see Fig. 8(e)] of the Pt atoms.

All these reconstruction geometries with bridging dimers and threefold- or fourfold-coordinated Pt atoms in Fig. 8 give rise to an energy gain with respect to the top Pt dimer geometries in Fig. 1. However, only the BDC model [Fig. 8(d)] may describe the observed dimerized-chain character of the Pt/Ge(001) surface. However, there are still too many Ge atoms in between the Pt chains in order to describe the observed significant corrugation in the quasi-1D overlayer.

V. TETRAMER-DIMER-CHAIN MODEL

A. Geometry and bonding

The energy gains (Table I) accompanying the formation of linear Pt chains together with top Ge dimers (BDC model) in Fig. 8(d) and the removal of Ge (SMR model) in Fig. 7(c) suggest further refinements, e.g., the removal of Ge atoms in the third atomic layer between two wires as indicated in Fig. 9. In addition, in this way we combine the idea of energy gain due to chains of fourfold-coordinated Pt atoms surround by Ge atoms with an idea to reduce the number of dangling bonds from the Ge(113) surface. At this surface tetramers, or better pentamers together with the fifth Ge atom in the third layer, appear.[44] The incorporated Pt atoms yield to alternating rows of twofold-coordinated (001)-like top Ge atoms

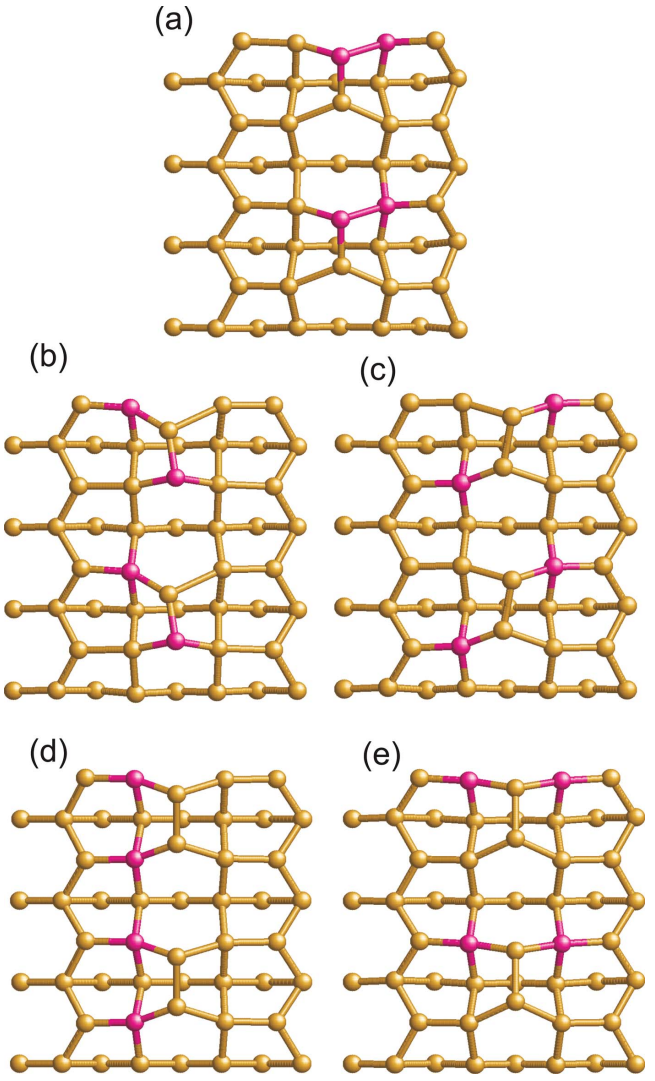

FIG. 8. (Color online) Dimerized Ge(001) surface with bridging dimers on top and two threefold- or fourfold-coordinated Pt atoms (dark or red spheres) replacing Ge atoms (bright or yellow spheres). The stick-and-ball models show the (a) BDN, (b) BDS, (c) BDA, (d) BDC, and (e) BDP structures.

with two dangling bonds and threefold-coordinated (111)-like Ge atoms below with one dangling bond. The pairing, even without dimerization, of the two topmost (001)-like atoms along the $[1\bar{1}0]$ direction leads to a $\times 2$ reconstruction. Together with two (111)-like atoms in almost $[1\bar{1}\bar{1}]$ direction the four atoms form a Ge tetramer. We have found that tetramers (or with the Ge atom in the third layer, pentamers) tend to open a gap[44] and therefore stabilize the (113) surface.

The combination of the structural elements, buried Pt (more precisely Pt-Ge) chains and tetramers together with Ge removal [see Fig. 7(c)], leads to the formation of wires with Ge top atoms as shown in Fig. 9(a). Because of the presence of Pt the tetramers remain almost symmetric, similarly to the situation for the clean diamond(113) surface.[44] The top pairs of Ge atoms practically do not show any buckling. The bonding situation is completely changed compared to the dimerized surface. The top Ge atoms do not form a dimer with a

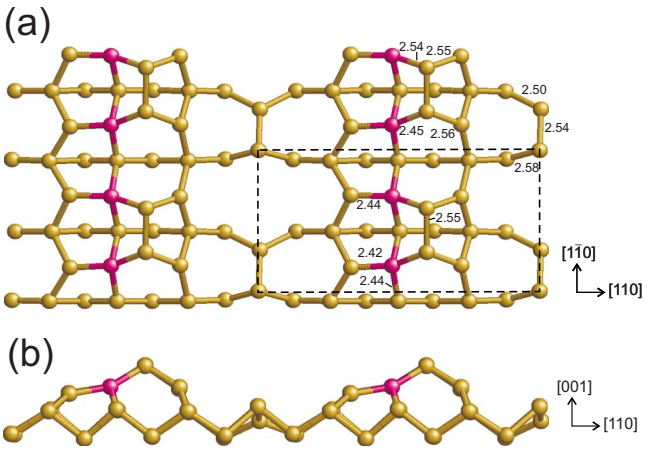

FIG. 9. (Color online) Top (a) and side (b) view of the tetramer-dimer-chain model of the Pt/Ge(001)4×2 surface with two Pt atoms per cell. The dark (red) circles represent Pt atoms, while the bright (yellow) ones stand for Ge atoms. A possible 4×2 surface unit cell is indicated by dashed lines. Lengths of important bonds are given in units of Å.

double bond. Rather, together with dangling bonds from the lower-lying tetramer Ge atoms, their dangling bonds form novel bonds and, hence, only represent the uppermost edge of a tetramer or pentamer.[44] The most important difference in Fig. 9 to the BDC model in Fig. 8(d) is the removal of second-layer Ge atoms between tetramers and Pt-Ge chains in $[1\bar{1}0]$ direction [see Fig. 9(b)]. This removal is energetically favorable for two reasons. First of all, it allows rebonding of four Ge dangling bonds in the form of buckled Ge homodimers in the third atomic layer. Moreover, it gives rise to additional degrees of freedom to adapt the surrounding bonds and hence to reduce the strain due to the incorporation of Pt atoms on Ge sites and the tetramer formation. Together with the Ge dimers in the trenches parallel to $[1\bar{1}0]$ a $4\times$ reconstruction appears in [110] direction.

The resulting tetramer-dimer-chain (TDC) model leads to a substantial energy gain in the grand canonical thermodynamical potential in Eq. (1) of about 2 eV/4×2 unit cell with respect to the reconstructions with top Ge dimers (Fig. 1).[21] The energy gain of about 0.25 eV/1×1 cell approaches the values known for the reconstruction of clean Ge surfaces.[39] We have also performed test calculations for a geometry similar to that given in Fig. 9. Only the topmost Ge pair per unit cell has been interchanged by the two Pt atoms in the buried Pt-Ge linear chains. However, as already demonstrated for the adsorbate geometries in Figs. 1 and 5, threefold-coordinated Pt atoms in on-top positions remain energetically less favorable. The occurring array of 1D structures is completely different compared with the conventional picture of dimerized Pt chains with Pt-Pt on top of the dimerized Ge(001) surface.[9,16–18] The resulting nanowires possess a complex bonding geometry. The topmost Ge atoms form linear ridges of dimerlike pairs (but only with a σ bond in wire direction) of tetramers. The Pt atoms give rise to evenly spaced linear chains without Pt-Pt bonds. In $[1\bar{1}0]$ direction, on the $[\bar{1}\bar{1}0]$ side, they are accompanied by parallel zigzag

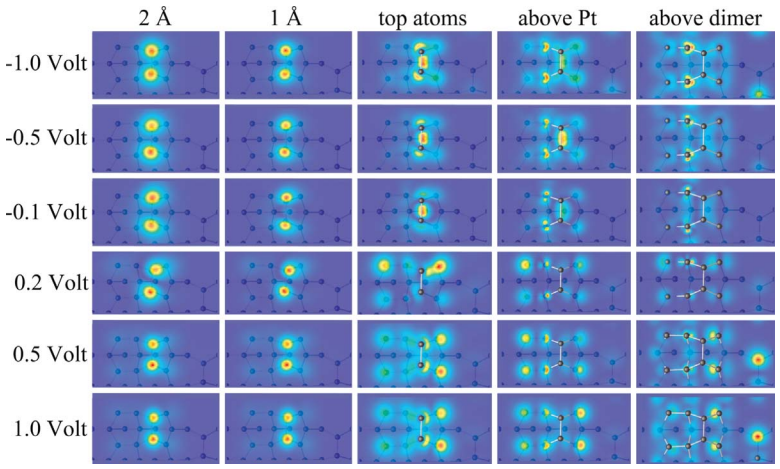

FIG. 10. (Color online) STM images simulated for the TDC model in a 4×2 unit cell for six bias voltages varying in the interval -1 V to $+1$ V. Negative (positive) voltages refer to occupied (unoccupied) states. The uppermost edge of the tetramer almost appears in the cell center. The atoms in the uppermost layers are indicated. The calculated constant-height images are plotted for planes 2, 1, or 0 Å above the top Ge atoms. Also lower planes just above the Pt atoms or the trench dimer are also shown.

chains of rebonded Ge atoms with one remaining dangling bond. The Pt chains on one side of the topmost Ge chains and the tetramers on the other side explain the subtle asymmetry perpendicular to the nanowires observed in STM images. Notably the top ridge of the wires is formed by Ge-Ge pairs, standing up high above the surface [see Fig. 9(b)], while the Pt atoms are located below. This will lead to seemingly almost symmetric dimerlike features in experimental STM overview images, especially since the top Ge-Ge pairs are strongly contributing to constant-current images discussed below. The proposal of an asymmetric reconstruction on a formerly symmetric substrate surface is also substantiated by the observation of phase and antiphase reconstructions in the experiment.[9,18]

The characteristic edge lengths of the rectangular unit cell are $2\sqrt{2}a_0\approx16$ Å and $\sqrt{2}a_0\approx8$ Å with an experimental cubic substrate lattice constant of about 5.68 Å. The vertical distance between the trench Ge dimers and the top Ge pairs amounts to about 4 Å. Within the DFT-GGA treatment these lengths are slightly overestimated by 1.7%. The Ge pairs in the top chain exhibit only a vanishing buckling. The same holds for the puckering tendency of the tetramer. However, the Ge dimers in the trenches between two wires (Fig. 9) show a remarkable buckling amplitude of about $\Delta z=0.84$ Å. Interestingly the short Pt-Ge bond lengths are varying between 2.42–2.54 Å in Fig. 9(a). They indicate strong bonds similar to the Ge-Ge ones. In any case they are much shorter than the Pt-Pt bonds shown in Fig. 1 and, hence, may be one of the reasons for the energy lowering within the TDC model. The Ge-Ge nearest-neighbor distances within the tetramers and in the trench dimer region vary between 2.50 and 2.58 Å somewhat larger than the bulk bond length. This fact has already been observed for the clean Ge(001)2×1 (Ref. 28) and Ge(113) (Ref. 44) surfaces. The strongest bond elongation is due to the trench dimer buckling. The accompanying strain-induced energy loss is however overcompensated by the energy gain by occupying Ge *s* instead of *p* states. The arrangement of buckled dimers makes a transformation into a $\times4$ reconstruction likely. A doubling of the unit cell to a $8\times$ reconstruction in the perpendicular direction is possible by an antiphase arrangement of the neighboring chains similar to the case of the In/Si(111)8×2 surface.[40,45] The increase in the chain distances from $2\sqrt{2}a_0$ to $3\sqrt{2}a_0\approx24$ Å (and consequently a 6×2 reconstruction) by a missing row defect, as observed,[18,20] is also possible by extending the trench region within the above described TDC model.

The understanding of the bonding and the occupation of surface electronic states is rather difficult because of the complexity of the Pt-induced TDC reconstruction. Figure 10 illustrates the surface orbitals and their occupation. Although it shows STM images for occupied and empty states close to the Fermi level but varying distance of the chosen constant-height plane, their development with the bias voltage and their location allow important conclusions about the electronic states. Within the TDC model the Pt/Ge(001) surface possesses 12 Ge dangling bonds (DBs) per 4×2 unit cell. Four DBs occur at the dimer atoms in the trench. Further four DBs are visible at the two topmost Ge atoms. Each of the two atoms at the lower base of the tetramer has one DB. The same is true for the lower Ge atoms adjacent to the Pt-Ge chain. Two DBs of the trench atoms and the topmost Ge atoms form σ bonds. The occupation of the buckled Ge dimer orbitals in the trenches is the same as for dimers on a clean Ge(001) surface. Because of the buckling one of the remaining (*s*-like) DBs is filled, whereas the other one (p_z-like) is empty. The two DBs belonging to Ge atoms adjacent to Pt atoms are almost empty because of the electron transfer toward Pt atoms. The remaining DBs at the topmost Ge atoms form bonding and antibonding combinations with the DBs of the Ge atoms at the tetramer base. The paired DBs remain more or less half-filled. However, due to the difference in *s* and *p* character of the remaining DB at a topmost atom and of the DB at a lower atom, there is a minor electron transfer from the lower Ge atom to the topmost one.

As a consequence of the geometry in Fig. 9 and the surface bonding discussed above one may formulate three main arguments for the drastic total-energy (more strictly: grand canonical potential) lowering within the TDC model compared to the models with top chains of Pt-Pt homodimers: (i) Because of the formation of buried Pt-Ge chains, each Pt atom leads to the formation of four Pt-Ge bonds instead of two Pt-Ge bonds and one Pt-Pt bond. (ii) The fourfold-coordinated Pt atom requires Ge atoms in positions more distant from the bulk. This leads to small (113)-like facets between topmost Ge atoms and trench atoms. It is well

known that atoms in different atomic layers with one or two DBs form a tetramer as the most stable reconstruction element on a (113) surface of group-IV semiconductors. Such tetramers make (113) surfaces to the second most stable faces at least more stable than (001) ones. (iii) Electron transfer from adjacent Ge dangling bonds into Ge-Pt bonds close to the Pt atoms.

B. STM images

How the atomic geometry in Fig. 9 is reflected in the electronic structure is demonstrated by the STM images in Fig. 10 simulated according to the Tersoff-Hamann method.[30] For the tip above the topmost surface layer, independent of the occupation of the states near the Fermi level, one only observes image maxima due to states localized at more or less symmetric Ge pairs. They seemingly indicate dimerized linear chains as claimed to be observed in the majority of STM experiments.[9,16,18,21] The relative constancy of the images is a consequence of the p-like dangling bonds forming bonding and antibonding combinations with dangling bonds at lower Ge tetramer atoms. The small asymmetries of the images for small bias voltages are probably a consequence of the reduced accuracy of the calculations in the energy range of only a few bands. As demonstrated below the density of states decreases for energies near the Fermi level so that the applied BZ sampling is probably not dense enough.

For planes crossing the top Ge atoms lying above the Pt atoms the images show drastic changes. The σ bond of the top Ge pair is clearly visible in the occupied-state image while the empty-state image is dominated by the corresponding antibonding as well as empty π orbitals localized at the lower Ge tetramer atoms and Ge atoms bonded to the buried Pt-Ge chains. However, also d-derived states at the Pt atoms are visible. For the lower-lying image plane the contribution of these Pt states is more significant in the occupied-state images. Here, in addition, also dangling bonds are visible at the remarkably buckled Ge dimers in the trenches.

Altogether, a more detailed analysis of the STM images as well as of the resulting differential conductivity and their comparison with experimental data in Ref. 21 suggests agreement and consequently the validity of the TDC model. As seen from Fig. 10 the constant-height images calculated for the TDC model can explain the important features seen in the experimental STM images for almost constant current. Among them are (i) the seemingly observation of dimerized linear chains (see two left panels in Fig. 10), (ii) the asymmetry of the wires perpendicular to the wire direction (see especially third and fourth panels for occupied states), and (iii) the vanishing dimerization and appearance of monomers for small bias voltages. In the calculated spectra this effect is (see left panels for −0.1 V) more visible for empty states. For occupied states the used BZ sampling seems to be not dense enough.

C. Electronic band structure

The band structure without spin-orbit coupling of the TDC surface (Fig. 9) which determines the STM images in Fig. 10 is plotted in Fig. 11(a) along high-symmetry lines $\Gamma-J-K-J'-\Gamma$ in the surface BZ.[39] The Fermi level is used as energy zero. DFT-LDA energies above 0.25 eV and below −0.40 eV essentially represent bulk bands projected onto the BZ of the Ge(001)4×2 surface. They are therefore of minor interest. Most interesting are the bands near the Fermi level. The two bands above and below the Fermi level show similarities with the surface bands of the diamond (111)2×1 surface within the π-bonded chain structure,[46] although the origin of these bands has nothing to do with bonding or antibonding combinations of π orbitals along the $[1\bar{1}0]$ direction. Nevertheless, the two bands around the Fermi level may similarly be traced back to chain structures parallel to the wire direction. Perpendicular to the chain orientation along JK and $J'K$ the bands are less dispersive. This holds especially along the JK line where the empty and occupied bands approach each other. The band structure basically describes an indirect zero-gap semiconductor with the maximum of the occupied band near K and the minimum of the empty surface band near J.

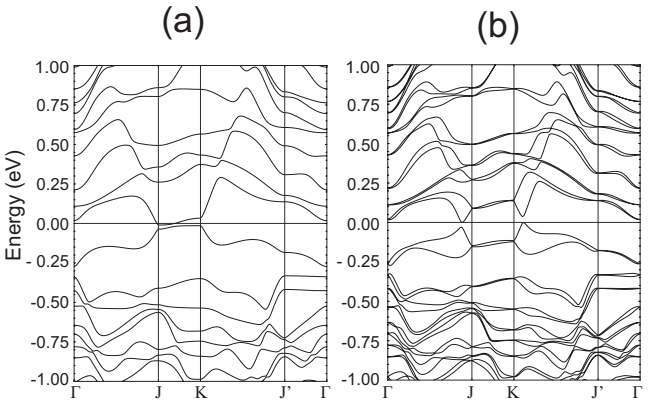

FIG. 11. Band structure for the tetrameter-dimer-chain model given in Fig. 9 without (a) and with (b) spin-orbit interaction. The Fermi level is used as energy zero.

The orbital character of certain band states near the Fermi energy in Fig. 11(a) is shown in Fig. 12. Apart from deeper atomic layers the state belonging to the lowest conduction band at a wave vector $\Gamma J/2$ [between Γ and J; see Fig. 12(a)] shows contributions from Pt states and empty dangling bonds at neighboring Ge atoms which have transferred their electrons to the Pt atoms. Close to the band minimum at J the electronic states [Fig. 12(b)] are really dominated by such localized in the top region of the quantum wire parallel to $[1\bar{1}0]$. One observes strong contributions of empty orbitals of the uppermost Ge ridge atoms and the adjacent Pt atoms. Near to the Γ point [Fig. 12(c)] the contributions from the Ge ridge atoms disappear totally. Probability to find an electron is now located at other Ge states, especially at the empty p-like orbital of the buckled Ge dimers between the wires.

The occupied states for wave vectors along the wire direction near $\Gamma J/2$ [between Γ and J; see Fig. 12(d)] and near $KJ'/2$ [between K and J; see Fig. 12(f)] have strong similarities with the probability to find an electron in the conduction band near J. The corresponding orbitals are however now governed by bonding combinations of Pt states and sp^3

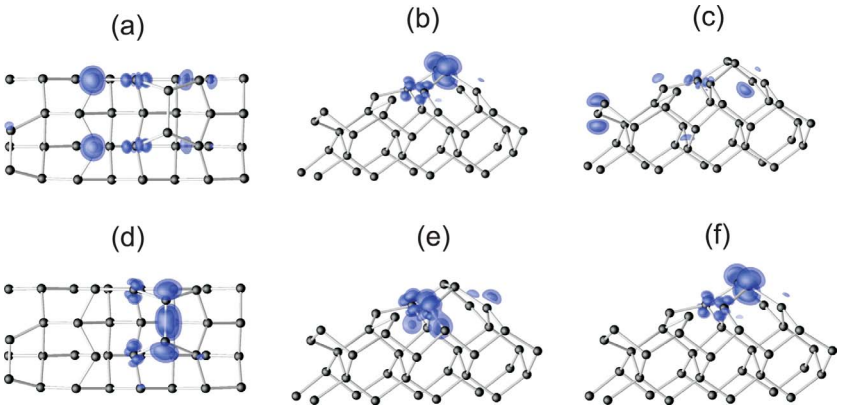

FIG. 12. (Color online) Top and perspective side views on wave-function squares of lowest conduction-(c) and valence (v)-band states at certain **k** points in the BZ as given in Fig. 11(a) (without spin-orbit coupling). (a) c at $\Gamma J/2$, (b) c at J, (c) c at Γ, (d) v at $\Gamma J/2$, (e) v at K, and (f) v at KJ'.

Ge orbitals located at atoms below the ridge tetramer atoms and σ bonds of the Ge ridge atoms. There are again drastic changes when varying to wave vectors perpendicular to the wire direction. Already the occupied states at the K points [Fig. 12(e)] exhibit a completely different orbital character. It is governed by bonding combinations of Pt atoms and Ge atoms between them in the next lower atomic layer.

The orbital characters of the lowest empty state at J [see Fig. 12(b)] and the highest occupied state at K [see Fig. 12(f)] indicate the important role of Ge ridge atom states as well as of Pt states for the nanowire conductivity. For electron transport near J besides Pt states especially states at Ge ridge atoms contribute [see Fig. 12(b)]. Electron transport in the wire direction may be related to a zigzag path along two Pt atoms with two Ge ridge atoms in between. The electron flow between two Pt atoms can only happen along Pt-Ge bonds and Ge-Ge top-ridge pairs. Two Pt atoms of a buried Pt-Ge zigzag chain are bridged by bonds to the ridge Ge atoms with an antibonding combination belonging to the σ bond in between. On the contrary, the hole transport near K is only determined by states along the buried chain of fourfold-coordinated Pt and Ge atoms in the second atomic layer as clearly visible from Fig. 12(e).

In the literature[13,47] the idea, that in contrast to $4d$ atoms the adsorption of noble $5d$ atoms tends to strong, more directional bonds including the $5d$ states with substrate atoms is a consequence of the much stronger relativistic effects, suggests to investigate the influence of such effects, especially the spin-orbit interaction. Therefore, the electronic band structure has also been calculated for an adsorbate system with TDC geometry (Fig. 9) including noncollinear spins and spin-orbit coupling. The results are shown in Fig. 11(b). Because of the high atomic number of 78 the spin-orbit splitting, e.g., that of the Δ_5 states in a Pt metal, may be on the order of 1 eV.[48] The band structure in Fig. 11(b) which has been calculated including the spin-orbit interaction however exhibits much smaller effects due to the mixing with Ge atoms. The $\Gamma_{25'}$ p-like valence states of bulk Ge (with a Ge atomic number of 32) give rise to a smaller spin-orbit splitting constant of about 0.3 eV.[37] However, from Fig. 11(b) it is clearly seen that the spin degeneracy along the high-symmetry lines outside the high-symmetry points is lifted. However, in general, the effect remains relatively small, in any case much smaller than the spin-orbit splitting of p states in bulk Ge. The strongest spin-orbit effect happens for the two close and parallel bands along JK near the Fermi level. Spin-orbit interaction leads to a coupling of the near four (including spin) band states along JK. As a result a significant repulsion of two (one occupied, one empty) groups of two bands around the Fermi level occurs. Their distance in Fig. 11(b) increases to a value of 0.2–0.25 eV. Due to spin-orbit-induced crossing and repulsion now gaps between occupied and empty bands appear on the ΓJ line near J as well as on the KJ' line near K, i.e., for wave vectors along the wire direction $[1\bar{1}0]$. The gap values amount to about 30 meV. Obviously a semiconductor with a small gap can be stated after inclusion of relativistic effects. In general, the spin-orbit effects lead to a reduction in the density of states for energies close to the Fermi level. The spin-orbit splitting of the uppermost valence band and the lowest conduction band for high-symmetry lines along the $[1\bar{1}0]$ wire direction leads not only to their mixing but also to a stronger **k** dispersion near J and K. The anticrossing effect has been computationally proven by a strong increase in the **k**-point mesh in wire direction to more than 200 **k** points in the contour. In summary, the principal character of the band structure is conserved after inclusion of the spin-orbit interaction. However, the top of the occupied surface band is displaced from K to a point close to K at the KJ' line. The minimum of the lowest empty surface band appears at a point on the $\Gamma J'$ line near the J' point. Gaps are opened and the lowest conduction bands and highest valence bands along JK are remarkably shifted against each other.

VI. SUMMARY AND CONCLUSIONS

In summary, using *ab initio* calculations for total energies and electronic structures we have studied quasi-one-dimensional nanowire arrays induced by low-coverage Pt adsorption on the Ge(001) surface. According to experimental results a 0.25-monolayer coverage and a 4×2 reconstruction have been investigated. In contrast to the number of Pt atoms, the number of Ge atoms in the surface slab has been allowed to vary. Experimental STM images suggest the existence of dimerized linear chains of Pt atoms on the Ge(001) surface. Indeed, such chains on top of each second Ge homodimer row or bridging two neighboring Ge dimer rows can roughly explain the observed overall STM images with exception of the asymmetry perpendicular to the wire direc-

tion. The resulting electronic structures represent a metallic surface or even an insulating surface with an extremely small gap.

The energy gain due to the formation of threefold-coordinated Pt atoms and one Pt-Pt bond per pair on top of the dimerized Ge(001) surface is much smaller than characteristic values for other reconstructed group-IV surfaces. Therefore, we have studied many other adsorbate structures. Tests of about 20 different surface geometries with different Ge contents suggest that Pt-Ge bonds are energetically more favorable than Pt-Pt bonds. Moreover, the minimization of the total free energy of the system obviously favors fourfold-coordinated Pt atoms. Simultaneously from the clean Ge(001) surface it is known that the number of Ge dangling bonds should be minimized by the formation of dimers or other reconstruction elements.

In order to bring the three tendencies for driving forces of the self-organization of quantum wires on the Ge(001) surface together, we started the construction of a more complex model of the quasi-one-dimensional chain structure due to Pt adsorption from the fact that the resulting spatially extended wires should possess facets which may locally be close to (113) ones. The corresponding surface orientation gives rise to low surface energy of the clean Ge(001) surface. The characteristic reconstruction elements are tetramers or even pentamers. The combination of all these ideas has allowed us to create a model for the quasi-one-dimensional chain array. The tetramer-dimer-chain model was found to lower significantly the total energy (more strictly the grand canonical potential) compared to the standard models with top linear Pt chains. It is mainly characterized by top chains of Ge pairs which are connected to fourfold-coordinated Pt atoms on one side and Ge tetramer atoms on the other side of the wire. Such a bonding geometry also explains the asymmetry of the observed STM images.

The accompanying electronic band structure represents an indirect zero-gap semiconductor, without inclusion of spin-orbit interaction. Spin-orbit splitting opens small gaps near the high-symmetry points J and K at the BZ boundary. The calculated STM images explain the experimental findings, at least taking the limitation to constant-height images in the theoretical description into account. The character of the states depends very much on the position in $\mathbf{k}$ space and especially on the energetical distance to the Fermi level. Near the Fermi energy Pt-derived electronic states play an important role. However, in the empty-state case they are superimposed by orbitals localized at the top-ridge Ge atoms. Consequently, Pt states strongly contribute to the nanowire conductivity despite the fourfold-coordinated position of the Pt atoms in the second atomic layer. Hole transport may be along the buried Pt-Ge chains while electron transport may be characterized by a zigzag movement of electrons approaching Pt chain atoms as well as topmost Ge atoms.

ACKNOWLEDGMENTS

We thank J. Schaefer and M. Wisniewski for helpful discussions. We acknowledge financial support from the Deutsche Forschungsgemeinschaft (Project No. Be1346/16-2) and the European Community in the framework of the Network of Excellence NANOQUANTA (Contract No. NMP4-CT-2004-500198). We gratefully acknowledge supercomputer time provided by the NIC Jülich.

*Permanent address: Q-Cells AG, OT Thalheim, Guardianstrasse 16, 06766 Bitterfeld-Wolfen, Germany.

[1] G. Grüner, *Density Waves in Solids* (Addison-Wesley, Reading, MA, 1994).
[2] J. M. Luttinger, J. Math. Phys. **4**, 1154 (1963).
[3] M. G. Zacher, E. Arrigoni, W. Hanke, and J. R. Schrieffer, Phys. Rev. B **57**, 6370 (1998).
[4] R. E. Peierls, *Quantum Theory of Solids* (Clarendon, Oxford, 1964).
[5] P. Segovia, D. Purdie, M. Hengsberger, and Y. Baer, Nature (London) **402**, 504 (1999).
[6] H. W. Yeom *et al.*, Phys. Rev. Lett. **82**, 4898 (1999).
[7] O. Bunk, G. Falkenberg, J. H. Zeysing, L. Lottermoser, R. L. Johnson, M. Nielsen, F. Berg-Rasmussen, J. Baker, and R. Feidenhansl, Phys. Rev. B **59**, 12228 (1999).
[8] R. Losio, K. N. Altmann, and F. J. Himpsel, Phys. Rev. Lett. **85**, 808 (2000).
[9] O. Gurlu, O. A. O. Adam, H. J. W. Zandvliet, and B. Poelsema, Appl. Phys. Lett. **83**, 4610 (2003).
[10] J. Wang, M. Li, and E. I. Altman, Phys. Rev. B **70**, 233312 (2004).
[11] J. N. Crain, J. L. McChesney, F. Zheng, M. C. Gallagher, P. C. Snijders, M. Bissen, C. Gundelach, S. C. Erwin, and F. J. Himpsel, Phys. Rev. B **69**, 125401 (2004).
[12] T. Tanikawa, I. Matsuda, T. Kanagawa, and S. Hasegawa, Phys. Rev. Lett. **93**, 016801 (2004).
[13] R. H. M. Smit, C. Untiedt, A. I. Yanson, and J. M. van Ruitenbeek, Phys. Rev. Lett. **87**, 266102 (2001).
[14] J. Wang, M. Li, and E. I. Altman, J. Appl. Phys. **100**, 113501 (2006).
[15] M. Kageshima, Y. Torii, Y. Tano, O. Takeuchi, and A. Kawazu, Surf. Sci. **472**, 51 (2001).
[16] N. Oncel, A. van Houselt, J. Huijben, A.-S. Hallbäck, O. Gurlu, H. J. W. Zandvliet, and B. Poelsema, Phys. Rev. Lett. **95**, 116801 (2005).
[17] O. Gurlu, H. J. W. Zandvliet, B. Poelsema, S. Dag, and S. Ciraci, Phys. Rev. B **70**, 085312 (2004).
[18] J. Schäfer, D. Schrupp, M. Preisinger, and R. Claessen, Phys. Rev. B **74**, 041404(R) (2006).
[19] O. Gurlu, A. van Houselt, W. H. A. Thijssen, J. M. van Ruitenbeck, B. Poelsema, and H. J. W. Zandvliet, Nanotechnology **18**, 365305 (2007).
[20] A. van Houselt, N. Oncel, B. Poelsema, and H. J. W. Zandvliet, Nano Lett. **6**, 1439 (2006).
[21] A. A. Stekolnikov, F. Bechstedt, M. Wisniewski, J. Schäfer, and R. Claessen, Phys. Rev. Lett. **100**, 196101 (2008).

[22] P. Hohenberg and W. Kohn, Phys. Rev. **136**, B864 (1964).
[23] W. Kohn and L. J. Sham, Phys. Rev. **140**, A1133 (1965).
[24] J. P. Perdew, in *Electronic Structure of Solids '91*, edited by P. Ziesche and H. Eschrig (Akademie-Verlag, Berlin, 1991), p. 11.
[25] J. P. Perdew, J. A. Chevary, S. H. Vosko, K. A. Jackson, M. R. Pederson, D. J. Singh, and C. Fiolhais, Phys. Rev. B **46**, 6671 (1992).
[26] G. Kresse and J. Furthmüller, Comput. Mater. Sci. **6**, 15 (1996); Phys. Rev. B **54**, 11169 (1996).
[27] G. Kresse and D. Joubert, Phys. Rev. B **59**, 1758 (1999).
[28] A. A. Stekolnikov, J. Furthmüller, and F. Bechstedt, Phys. Rev. B **65**, 115318 (2002).
[29] H. J. Monkhorst and J. D. Pack, Phys. Rev. B **13**, 5188 (1976).
[30] J. Tersoff and D. R. Hamann, Phys. Rev. B **31**, 805 (1985).
[31] M. S. Hybertsen and S. G. Louie, Phys. Rev. B **34**, 5390 (1986).
[32] F. Bechstedt, Adv. Solid State Phys. **32**, 161 (1992).
[33] W. G. Aulbur, L. Jönsson, and J. W. Wilkins, *Solid State Physics: Advances in Research and Applications* (Academic, San Diego, 2000), Vol. 54, p. 1.
[34] U. von Barth and L. Hedin, J. Phys. C **5**, 1629 (1972).
[35] D. Hobbs, G. Kresse, and J. Hafner, Phys. Rev. B **62**, 11556 (2000).
[36] R. Enderlein and N. J. M. Horing, *Fundamentals of Semiconductor Physics and Devices* (World Scientific, Singapore, 1997).
[37] M. Cardona, K. L. Shaklee, and F. H. Pollak, Phys. Rev. **154**, 696 (1967).
[38] W. B. Pearson, *Crystal Chemistry and Physics of Metals and Alloys* (Wiley, New York, 1972).
[39] F. Bechstedt, *Principles of Surface Physics* (Springer, Berlin, 2003).
[40] X. Lopez-Lozano, A. Krivosheeva, A. A. Stekolnikov, L. Meza-Montes, C. Noguez, J. Furthmüller, and F. Bechstedt, Phys. Rev. B **73**, 035430 (2006).
[41] K. Miki, D. R. Bowler, J. H. G. Owen, G. A. D. Briggs, and K. Sakamoto, Phys. Rev. B **59**, 14868 (1999).
[42] J. H. G. Owen, K. Miki, and D. R. Bowler, J. Mater. Sci. **41**, 4568 (2006).
[43] Sargent-Welch, *Table of Periodic Properties of the Elements* (Sargent-Welch Scientific, Skokie, 1980).
[44] A. A. Stekolnikov, J. Furthmüller, and F. Bechstedt, Phys. Rev. B **67**, 195332 (2003); **68**, 205306 (2003).
[45] A. A. Stekolnikov, K. Seino, F. Bechstedt, S. Wippermann, W. G. Schmidt, A. Calzolari, and M. Buongiorno Nardelli, Phys. Rev. Lett. **98**, 026105 (2007).
[46] M. Marsili, O. Pulci, F. Bechstedt, and R. Del Sole, Phys. Rev. B **72**, 115415 (2005).
[47] Abu Md. Asaduzzaman and M. Springborg, Phys. Rev. B **72**, 165422 (2005).
[48] A. Dal Corso and A. Mosca Conte, Phys. Rev. B **71**, 115106 (2005).